ISSN 0208-7774 TRIBOLOGIA 1/2020 p. 63–73
DOI: 10.5604/01.3001.0014.0852

Anna Maria RYNIEWICZ[*], Andrzej RYNIEWICZ[**]

ANALYSIS OF THE MECHANISM OF LUBRICATION OF THE TEMPOROMANDIBULAR JOINT

ANALIZA MECHANIZMU SMAROWANIA STAWU SKRONIOWO-ŻUCHWOWEGO

Key words: CT and MRI model, modeling, MES simulations, biorheology, tribology, TMJ.

Abstract: The aim of the work is to identify the lubrication conditions of the correct temporomandibular joint (TMJ) based on spatial modeling of joint structures, load simulations, reduced stresses, and resultant deformations in correlation with rheological parameters of synovial fluid. The material used in this study is the results of normal joint imaging performed using a standardized technique under occlusal conditions. Modeling and the simulation of contact, after the introduction of strength parameters of hard tissues, fibrous cartilage, and synovial fluid and the imposition of boundary conditions was carried out in the following program: Femap NE Nastran. Spatial simulation of contact between joint structures, virtual loading, and the visualization of what happens in the joint allows one to identify these structures in terms of tribology and strength. The transfer of loads in TMJ results from the geometric form of the supporting bone structures and joint surfaces, the distribution of the cartilage tissue building these surfaces, the geometry of the disc, and rheological parameters of the joint synovial fluid. In normal and loaded TMJ, differential displacement occurs in the joint cavity and cartilage structures, which stimulates the lubrication mechanism and optimize the use of synovial fluid properties. The joints are characterized by the absorption of maximum stresses reduced by bone structures. Load compensation and suspension is achieved by cartilage covering the joint surfaces and, to a large extent, by the joint disc and elastic-viscous response of a synovial fluid.

Słowa kluczowe: model CT i MR, modelowanie, symulacje MES, bioreologia, tribologia, SSŻ.

Streszczenie: Celem pracy jest identyfikacja warunków smarowania prawidłowego SSŻ na podstawie przestrzennego modelowania struktur stawowych, symulacji obciążeń, naprężeń zredukowanych i odkształceń wypadkowych w korelacji z parametrami reologicznymi cieczy synowialnej. Materiałem badań są wyniki obrazowania stawów prawidłowych wykonane w standaryzowanej technice w warunkach okluzji. Modelowanie i symulacje kontaktu, po wprowadzeniu parametrów wytrzymałościowych tkanek twardych, chrząstki włóknistej i cieczy synowialnej oraz nałożeniu warunków brzegowych, zrealizowano w programie Femap NE Nastran. Przestrzenna symulacja kontaktu struktur stawowych, wirtualne obciążanie i wizualizacja tego, co następuje w stawie, pozwala identyfikować te struktury w aspekcie tribologicznym i wytrzymałościowym. Przeniesienie obciążeń w SSŻ wynika z formy geometrycznej oporowych struktur kostnych i powierzchni stawowych, z rozkładu tkanki chrzęstnej budującej te powierzchnie, geometrii krążka oraz parametrów reologicznych mazi stawowej. W prawidłowym i obciążonym SSŻ pojawiają się w jamie stawowej oraz w strukturach chrzęstnych zróżnicowane przemieszczenia wypadkowe, które stymulują mechanizm smarowania i optymalizują wykorzystanie właściwości płynu synowialnego. Dla stawów charakterystyczne jest przejmowanie maksymalnych naprężeń zredukowanych przez struktury kostne. Kompensacja obciążenia i jego amortyzacja realizowana jest poprzez chrząstkę pokrywającą powierzchnie stawowe oraz w znacznym stopniu przez krążek stawowy i odpowiedź sprężysto-lepką cieczy synowialnej.

[*] ORCID: 0000-0003-2469-6527. Jagiellonian University Medical College, Faculty of Medicine, Dental Institute, Department of Dental Prosthodontics, Montelupich 4 Street, 31-155 Cracow, Poland.
[**] ORCID: 0000-0002-9140-198X. State University of Applied Science, Institute of Technology, Zamenhofa 1a Street, 33-300 Nowy Sącz, Poland.

INTRODUCTION

The temporomandibular joint (TMJ), unlike other joints in our system, is characterized by the fact that it is the only even joint. The jaw heads are functionally coupled with the mandibular body and its branches. The joint is composed of the joint fossa (acetabulum) within the temporal bone (a flat cavity at the back end of the zygomatic process with the protruding joint condyle) and the joint head on the condylar process of the mandible (**Fig. 1**).

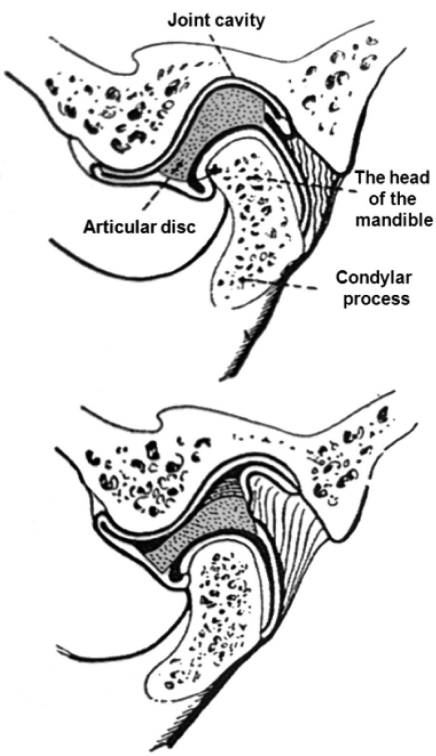

Fig. 1. Cross-section of the temporomandibular joint: a) in contraction, b) with the abducted mandible [L. 1]

Rys. 1. Przekrój stawu skroniowo-żuchwowego: a) w zwarciu, b) z odwiedzioną żuchwą **[L. 1]**

There is a joint disc between these structures. It divides the joint into two separate spaces in such a way that, although they do not connect directly with each other, they act together forming a single functional system. In recent years, as a result of advances in research methodology, some views on the structures and functions of the stomatognathic system (SS), including temporomandibular joints and chewing muscles, have changed **[L. 2–9]**. The work of temporomandibular joints is controlled by the lateral (disc), and capsular and temporomandibular ligaments. The fibres of the deep masticator muscle and temporal and superior lateral pterygoid muscles may penetrate the joint disc. The articular disc plays an important role in the physiology and function of joints. The basic role of joint discs is to enable complicated joint movements. Biomechanics of joints allows for speech articulation and food intake and chewing. Along with individual development, during the change in the way of taking and grinding food – from sucking to chewing – and the emergence of teeth in the oral cavity, there is a reconstruction of the joint structures.

In the SS, the main dynamic system is the mandible with the muscular and temporomandibular joint system, and its movements are controlled by stimuli sent from nerve endings in the periodontium, muscles, and the temporomandibular joints, and from the mucous membrane of the oral cavity and tongue. Three types of movements are performed smoothly in TMJ. When the mouth is opened and closed by a hinged movement, the heads of the jaws rotate about a mobile transverse axis. This axle moves forwards when opening and backwards when closing. The head of the mandible not only rotates hinged, but also slides along the joint disc, so there is no fixed pivot point. The mandible can move forward and in this sliding motion. The joint disc and the mandibular head can also slide forwards and backwards, even without opening the mouth. The range of this movement is about 15 mm. Grinding movement consists in the rotation of the mandible around the vertical axis. The head of the mandible slides forward, and the opposite head rotates around its vertical axis. These three types of movements are characteristic of human temporomandibular joints and are of biomechanical forces and adaptation to SS functions. The joint is surrounded by a joint capsule. From the top, it connects with the temporal bone, and while covering the joint surface of the lower and joint nodules, it reaches from the back to the petrotympanic fissure, while from the bottom, it surrounds the joint surface of the head of the mandibular condylar process. The joint capsule is reinforced with fibres that form ligaments running from the front and top, from the temporal bone to the bottom, and back to the condylar process of the mandible (the temporomandibular ligament). The entire circumference of the joint disc is connected to the joint capsule and the condylar process of the head of the mandible with medial and lateral collateral ligaments, which divide the joint into upper and lower floors (**Fig. 2**).

There are two connective tissue bands inside the joint stabilizing the position of the disc. The medial part of the disc is directly or indirectly penetrated by muscle fibres of the superior lateral pterygoid muscles, which attach themselves to the sphenoid bone and run towards the back and bottom of the mandible head. The superior lateral pterygoid muscles work asynchronously in relation to the inferior lateral pterygoid muscles. The superior lateral pterygoid muscles are active during the contraction of the mandible in relation to the maxilla. These muscles centrally position the mandibular head in the joint fossa and also show little activity while keeping

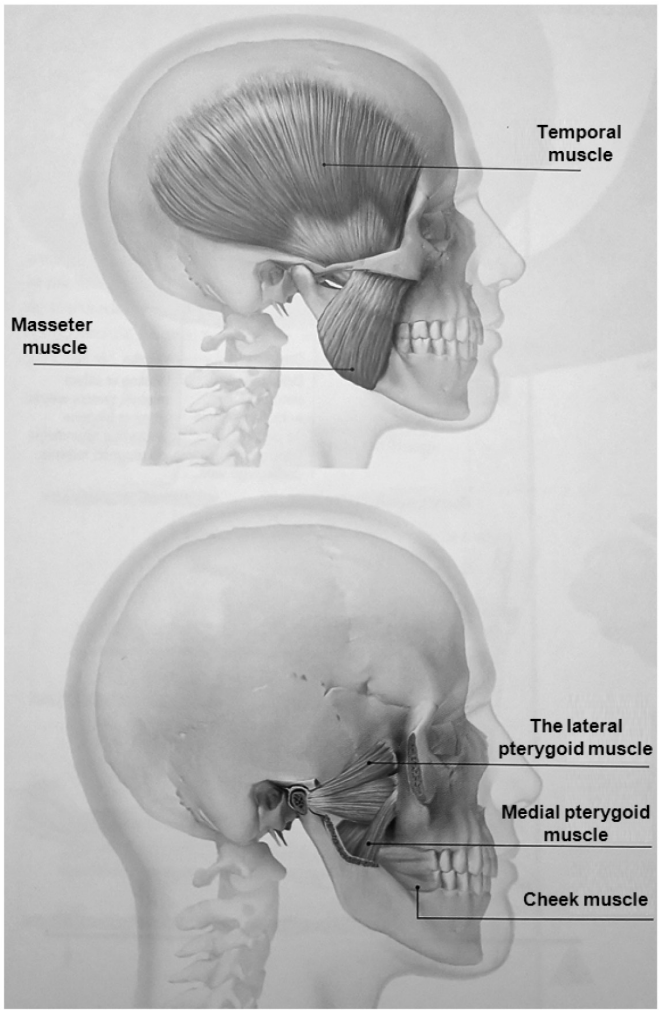

Fig. 2. Muscles involved in chewing [L. 10]
Rys. 2. Mięśnie biorące udział w żuciu **[L. 10]**

the mandible at rest. The analysis of TMJ preparations also revealed the penetration of fibres from the deep masseter muscle parts into the outer part of the joint discs and temporal muscle fibres into the inner parts of the discs **[L. 10]**. These muscles are referred to as active tensioning discs, which generate contact normal pressures and protect the joint fossa from pathological overloading of its cartilage and tissues located deeper in the temporal bone.

Another adaptation of the TMJ joint to the function of a perfect bearing is the presence of synovial fluid. The inner layer of the joint capsule is a synovial membrane producing synovial fluid. This liquid is located on both levels of the joint, moisturizes the joint surfaces on the principle of physical and chemical adsorption, and nourishes them by penetrating the cartilage on the principle of diffusion and chemical bonds **[L. 11–14]**. It also absorbs unnecessary metabolites. Synovial fluid is formed as an exudate from the synovium. Its flow is regulated by the pressure difference between the blood and the joint cavity, in which negative atmospheric pressure prevails. The fluid viscosity is determined by the content of 1–2% glycosaminoglycans. Glycosaminoglycans are multiparticulates polymers made of disaccharide repeating units consisting of hexosamine, glucosamine or galactosamine and uronic, glucuronic or iduronic acid linked by a glycosidic bond **[L. 15, 16]**. A characteristic feature is the presence of sulphate groups with the exception of hyaluronic acid. Hyaluronic acid belongs to the group of saccharide biopolymers with molecular weight from 500,000 to 700,000 D and protein content below 0.2%. This compound provides viscoelastic properties of synovial fluid and cartilage tissue. In complexes with proteoglycans and proteins, it plays the role of a mechanical buffer protecting chondrocytes against crushing **[L. 16]**. Synovial fluid owes its rheological characteristics, not only to its chemical structure, but also to the spatial configuration of hyaluronic acid and protein complexes. The synovial tests presented in the publication were preceded by a number of different rheological synovial tests and experiments performed

by the authors **[L. 15–17]**. They were carried out using synovial fluid respirated from the joint cavity from human joints (knee and upper ankle joints) and from pig joints (hip, knee, and temporomandibular joints). Rheological tests confirmed elastic-viscous properties of synovial fluid **[L. 15, 17]**. In addition to the typically viscous characteristics of liquids, elastic-viscous fluids also exhibit elastic properties typical of solids.

The aim of the work is to identify the lubrication conditions of the correct temporomandibular joint based on spatial modeling of joint structures, load simulations, reduced stresses, and resultant deformations in correlation with rheological parameters of synovial fluid. The joint lubrication mechanism is not replicated in technical nodes due to very low resistance to motion (coefficient of friction 0.001–0.005), at low speeds (0.01––0.05 m/s) and very high contact pressure (20–80 MPa). Attention should be paid to the long-term operation of bio-bearings, with a minimum of wear products.

MATERIAL AND METHOD

The material of the study is a model of left TMJ of a man (aged 30) reconstructed on the basis of CT and MR imaging. Imaging examinations were carried out in the Diagnostic Imaging Laboratory of the John Paul II Hospital in Cracow. A reference position is used in both imaging procedures. This position was characterized by the fact that the joint disc was located on the head of the joint and was in contact with the surface of the joint fossa with its thinnest part, and only a rotational movement around the stable hinge axis occurred in the joint **[L. 18, 19]**. CT imaging was performed with a Siemens Somation Cardiac spiral 64-layer CT scanner. MR imaging was performed with a Siemens Magneton Sonata Maestro Class device. A 3D model of joint bone structures was determined based on the CT scan. The model was supplemented on the basis of the MRI by cartilage and fibrous structures, which comprise the joint surfaces and the disc. Modeling and calculations were performed in the Femap NE Nastran program.

The joint surface of the condylar process is located mainly on the anterior surface of the mandibular head. It is covered with fibrous cartilage. The posterior surface of the joint head is located inside the joint capsule, but surrounded by elastic connective tissue. The dorsal portion covering the posterior surface of the joint head is divided into two layers:

– Upper layer – formed of loose connective tissue with nerves and capillaries, and
– Lower layer – formed of elastic connective tissue, is connected to the periosteum of the posterior surface of the mandibular neck.

The joint disc divides the joint cavity into the superior and inferior fissure. The middle part of the disc is made of elastic connective tissue, while the periphery of the disc contains cartilage cells. During the mandible's movements, the joint disc moves and acts as a movable acetabulum. The TMJ proper acetabulum lies on the lower surface of the zygomatic arch. It is positioned slightly diagonally in relation to the joint surface of the mandibular head, from which it is 2–3 times larger. The front of the joint surface is formed by the articular condyle. The lower jaw is loaded through the joint head only in the front part. The front part of the bottom is covered with fibrous cartilage. The developed model of correct TMJ allows for the analysis of joint structures (**Fig. 3**).

Biomechanical and tribological interactions were imposed on the model **[L. 15, 17]**. The articular surfaces of the condylar process and the joint fossa have been permanently bonded to the bone structures. The back of the disc is attached to a loose, vascularized connective tissue called *retrodiscal*, which attaches to the posterior wall of the joint capsule. From the medial and lateral side, it is firmly attached to the poles of the condylar process. From the front, it is connected with the joint capsule and the superior attachment of the lateral pterygoid muscle. Therefore, the modelled disc is permanently fixed to the medial and lateral poles of the condylar process and is resiliently fixed with the posterior and posterior edges. The joint fluid produced by the inner layer of the joint capsule is located in two joint cavities permanently separated by a disc. In the synovial fluid filling the joint cavities, the possibility of slipping was modelled. Contact with the introduction of a friction coefficient μ=0.005 was modelled between the articulating surfaces of the joint and the fluid **[L. 15]**. The attachments were placed on the temporal bone (**Fig. 4**).

Loads of 1000 N in parallel direction to the mandibular branch were applied on the mandibular head. This is the load corresponding to the contraction **[L. 15]**.

Due to biomechanical excitations occurring in TMJ and a specific lubrication mechanism, rheological tests of synovial fluid were carried out. The aim of the study was to determine the viscous and elastic properties of synovial fluid in vitro. These studies may be an indication to explain the excellent mechanism for lubricating biobearings **[L. 16]**.

The rheological tests presented in this study were performed using synovial fluid from temporomandibular animal joints with no signs of pathology. During sample preparation, care was taken that the fluid did not undergo denaturation, which may be caused by changes in temperature as well as pH, and that no loss of water from the fluid would occur during compression. The rheological examination fluid in the amount of 0.5 cm^3 was taken with a puncture syringe with a capillary diameter of 0.9 mm immediately before each measurement. 10 fluid samples were taken for oscillatory tests at variable frequency and constant deformation, and 10 samples were tested at variable

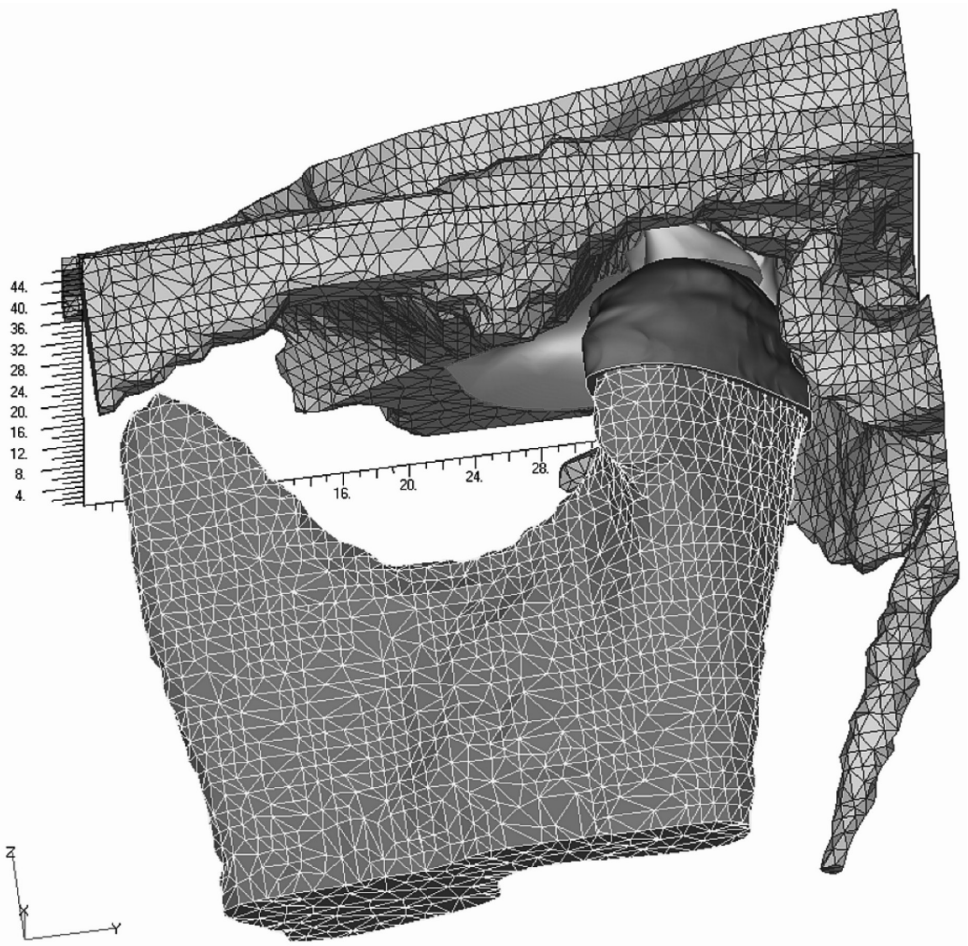

Fig. 3. Numerical model of the temporomandibular joint [L. 15]
Rys. 3. Model numeryczny stawu skroniowo-żuchwowego **[L. 15]**

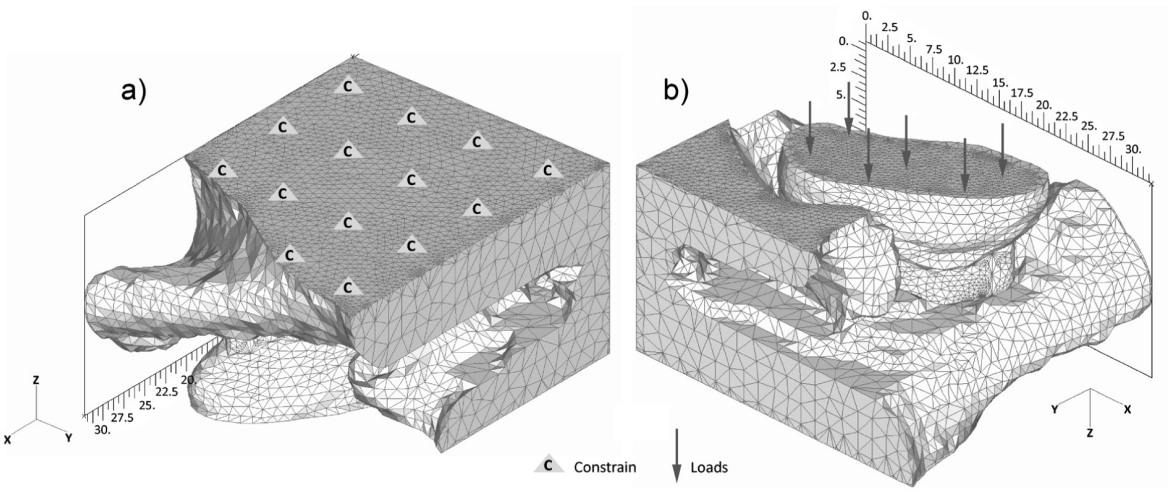

Fig. 4. Numeric model of TMJ with preset: a) constrain, b) loads [L. 15]
Rys. 4. Model numeryczny SSŻ z zadanymi: a) utwierdzeniami, b) obciążeniami **[L. 15]**

deformation and constant frequency. The research was carried out on an Anton Paar – Physica 501 rotational rheometer in a isothermal laminar drag flow (Conette) system in the gap between the rotating cone and the stationary plate at a temperature of 36.6°C. The cone-plate measuring system enables measurements in which shear stress and shear rate have a constant value – in the entire gap. This system is more often used to study the rheological properties of elastic-viscous fluids. The rheometer used allowed the determination of the flow curve, i.e. the relationship of shear stress to shear rate. This relationship characterizes the viscous properties of synovial fluid. To identify its elastic features, normal stress measurements were taken under oscillatory flow conditions that model biomechanical excitations in the SS under occlusion. Loads are transferred by joints in the range of low tangential speeds from 0.01 m/s to 0.5 m/s. For this range, the range of synovial shear rate was determined in rheological measurements. Research on cadavers' preparations shows that the thickness of the lubricating film in the gaps of biobearings is in the range from 0.32 μm to 800 μm. A 20 mm cone with an angle of 5 degrees was used in the measurements; as a result, the gap along the radius was 35 μm in the flattened central part around the top of the cone and 910 μm on its edge.

The results were values characterizing elastic and viscous properties. The elastic properties of the fluid were characterized by the conservative modulus G' and the viscous properties by the loss modulus G". These are the two main parameters characterizing the fluid in conditions of oscillating changing stresses/deformations.

Descriptive statistics were determined. The mean value and standard deviation were calculated, and the standard errors as well as the minimum and maximum values were determined.

RESULTS AND DISCUSSION

After MES calculations, the reduced stresses were visualized according to the HMH hypothesis and the resultant displacements. Reduced stresses in normal TMJ are differentiated, and their maximum values reach 10 MPa and are located in the bone structures of the head, partly in the area of the joint disc and in the subchondral and bone areas of the joint fossa (**Fig. 5**).

Accidental movements are also differentiated within the joint structure (**Fig. 6**). The maximum displacement values are up to 90 μm and occur in the posterolateral zone of the mandibular head. They are cushioned in contact with the head cartilage and the joint disc, and the cartilage that covers the joint bottom in such a way that they decrease to zero in temporal bone structures. The greatest gradient of displacement occurs in the lower joint cavity: 38 μm–65 μm, which can stimulate the lubrication mechanism by moving the synovial fluid in the disc/condylar zone. As a result of displacements, the size of the gaps changes, which translates into the occurrence of pressure changes in the synovial fluid. In the structure of the joint disc, the decrease in displacement is differentiated from 65 μm in the lower layers to 28 μm in the upper layers. In the disc and temporal cavity, the displacements remain within the range of 16 μm–28 μm. In the bone structures of the zygomatic process, it drops to zero. The results of simulation studies indicate a significant variation of stresses and displacements in the structure of the temporomandibular joint under static conditions. They result from the specific layered structure of the analysed biosynthesis, from the geometric shaping of joint surfaces (geometric form of the surface – the presence of gaps, the distribution of cartilage tissues building these surfaces, resistance form of bone layers), and the joint disc, as well as from the strength parameters of joint-forming tissues.

The fusion of CT and MRI imaging made it possible to identify bone and soft structures in TMJ **[L. 2, 3, 20–22]**. The modeling and simulation of a contraction allowed the determination of different stress distributions of reduced and resultant displacements. Their values do not exceed the physiological capacity of the tissues in contact **[L. 7–9, 23–27]**. They stimulate the lubrication mechanism in terms of anatomical structure. This is not the end of the adaptation of TMJ to the perfect lubrication mechanism. Biomechanical, physiological, and rheological adaptation of this biobearing to tribological processes was analysed in the conducted studies **[L. 8, 9, 11, 12, 27–33]**.

In order to determine the elastic properties of synovial fluid, oscillatory measurements were performed, which consisted in subjecting the samples to a sinusoidal changing stress or strain.

The measured values were the following: conservative module G', which represents the amount of energy stored by the sample and is a measure of the elastic properties of the fluid, loss module G", associated with energy dissipation and characterizing the viscous properties of the fluid and complex viscosity of synovial fluid (|η*|). Performing these measurements allowed the characteristics of elastic-viscous properties in the time scale range – low frequencies mean long times, and high frequencies – short deformation times (Fig. 7). The test was carried out twice with the same excitations for the same liquid sample. The results of the oscillatory measurements of the synovia are stable, and the next test has curves of elastic response G', viscous response G", and complex viscosity |η*| – shifted to higher values. The synovial rheological response stabilized at a frequency of 0.3 s^{-1}. The elastic response G′ was 8–9 Pa, and the viscous response G" was 6–9.2 Pa, whereas complex viscosity |η*| 25–33 Pa. As the frequency increased to 100 s^{-1}, the elastic response G' was 14–15 Pa, and the viscous response G" was 8.5–10.2 Pa, and complex viscosity |η*| 0.75–0.95 Pa•s. The increasing effect of

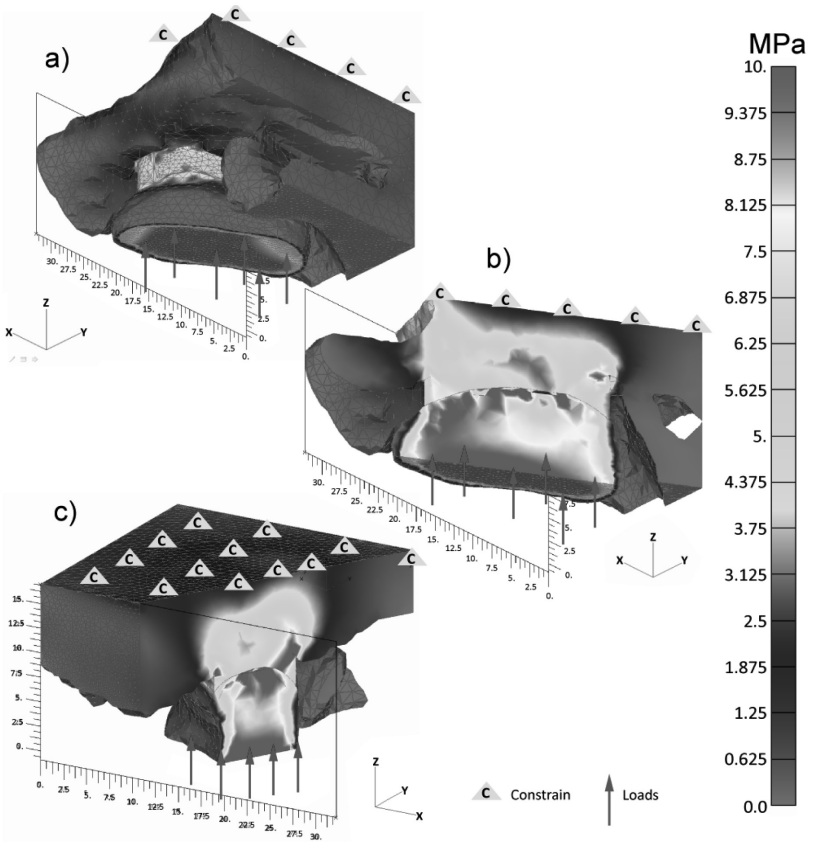

Fig. 5. Distribution of reduced stresses in normal TMJ: a) view in the coronal plane of the skull, b) cross-section of the plane passing through the medial and lateral poles of the mandibular head, c) cross-section of the sagittal plane through the centre of the mandibular head [L. 15]

Rys. 5. Rozkład naprężeń zredukowanych w prawidłowym SSŻ: a) widok w płaszczyźnie wieńcowej czaszki, b) przekrój płaszczyzną przechodzącą przez bieguny przyśrodkowy i boczny głowy żuchwy, c) przekrój płaszczyzną strzałkową przez środek głowy żuchwy **[L. 15]**

the elastic response was found. The increasing values of the conservative module G′ testify to the formation of a gel structure with elastic properties in a synovial fluid.

The oscillation tests of liquids carried out at variable deformation and constant frequency confirmed the significant dominance of the elastic response G 'over the viscous response G" and the persistent stability of these responses with increasing deformation (**Fig. 8**). The elastic response G ’remained at 21.5 Pa and the viscous response G" at 7.6 Pa.

Joint fluid exhibits elastic-viscous properties when the surfaces move relative to each other and when they are subjected to stresses below the flow limit. The fluid generates normal stresses, which prevent direct contact between the cooperating joint surfaces. Rheological tests confirmed the mechanism of fluid curing at deformations and the mechanism of normal stress generation, which play an important role in the process of contact load transfer, cartilage protection against wear, and chondrocyte protection against crushing **[L. 34, 35]**.

The actual flow of synovial fluid deviates from the conditions of the tests carried out. The elastic response of synovial fluid in TMJ occurs in two joint gaps, between anatomically shaped and covered with fibrous cartilage surfaces.

The areas of tribological cooperation are the following:

- Upper floor – articular gap formed between the articular surface in the temporal bone and the articular disc,
- Lower floor – articular gap formed between the disc and the articular head on the condyles of the mandible.

To date, there are no instruments that would allow measurement of rheological properties of synovia in vivo. The use of high resolution rheometer for research allowed the analysis of phenomena in the area of shear rates close to zero, which can explain the adaptation of synovial joints to carry heavy loads under static conditions and at low shear rates.

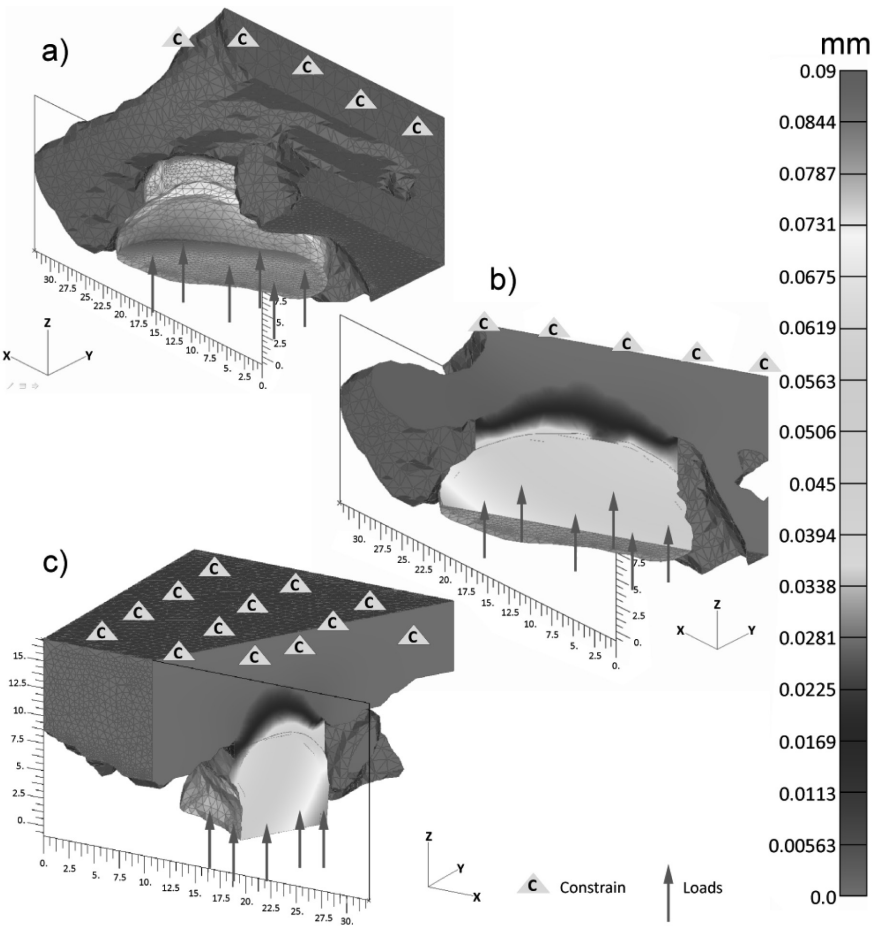

Fig. 6. Distribution of resultant displacements in normal TMJ: a) view of the coronal plane of the skull, b) cross-section of the plane passing through the medial and lateral poles of the mandibular head, c) cross-section of the sagittal plane through the centre of the mandibular head [L. 15]

Rys. 6. Rozkład przemieszczeń wypadkowych w prawidłowym SSŻ: a) widok w płaszczyźnie wieńcowej czaszki, b) przekrój płaszczyzną przechodzącą przez bieguny przyśrodkowy i boczny głowy żuchwy, c) przekrój płaszczyzną strzałkową przez środek głowy żuchwy **[L. 15]**

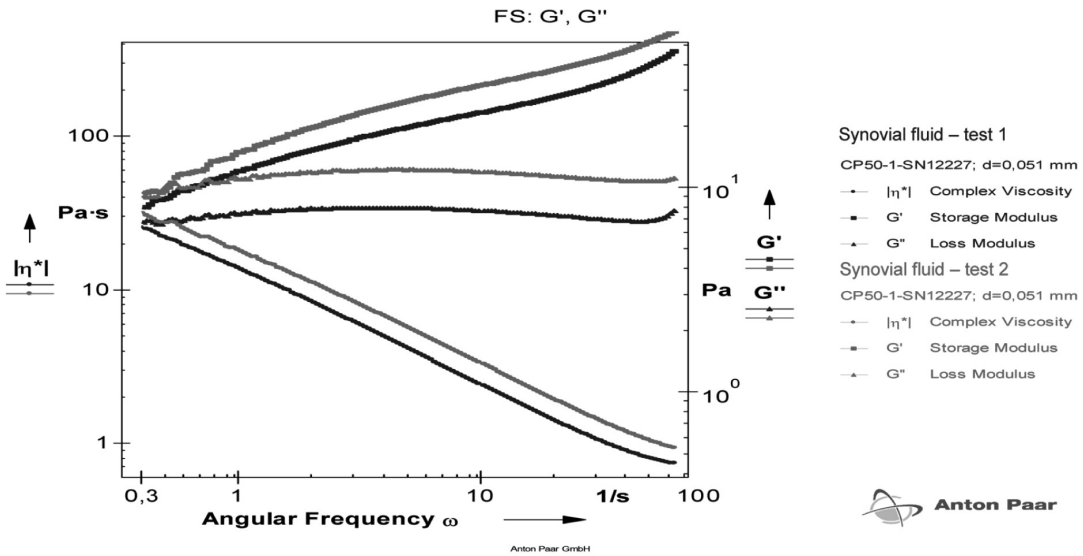

Fig. 7. Results of synovial fluid oscillation measurements at variable frequency and constant deformation

Rys. 7. Wyniki pomiarów oscylacyjnych cieczy synowialnej przy zmiennej częstotliwości i stałym odkształceniu

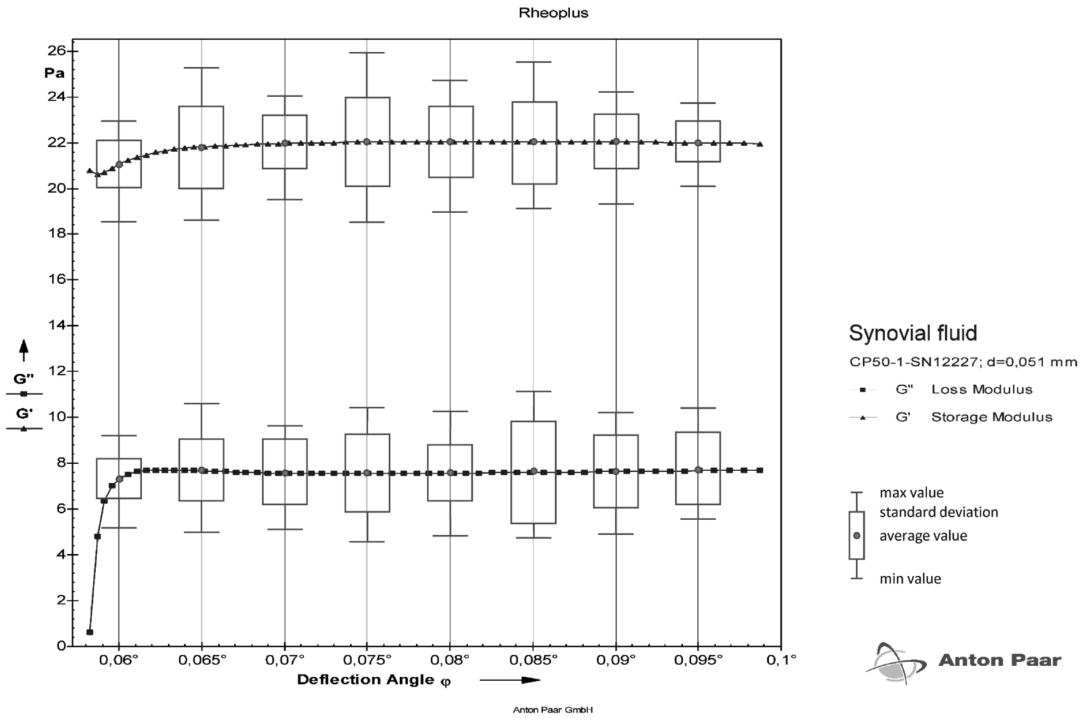

Fig. 8. Results of oscillatory measurements of synovial fluid at variable deformation and constant frequency
Rys. 8. Wyniki pomiarów oscylacyjnych cieczy synowialnej przy zmiennym odkształceniu i stałej częstotliwości

The technique of oscillatory testing involves subjecting the sample to a stress or deformation that changes sinusoidally and recording this reaction. Such tests have this valuable property, compared to steady-state tests that they do not affect the structure of the test substance as long as the deformation is sufficiently small. So they can be used to control processes that take place in a sample over time, because they leave the sample in the same condition it was in before the test. Structural violations always occur during a constant viscometric flow, because, during such a measurement, the deformation reaches much higher values than in the case of deformations used in oscillatory tests.

According to our theory about the excellent lubrication mechanism of TMJ, in addition to shape adaptations (disc accommodation – formation of lubricating wedges, acetabulum and head), strength properties of fibrous tissue, tissue distribution on joint surfaces, the nature of tribological excitations, the biomechanics of the muscular syndrome, fluid production through the synovium, the presence of chondrocytes, the elastic response of synovial fluid is essential. The determined elastic response values are characteristic of this liquid and do not find replication in other lubrication media in technical conditions. The stimulator of elastic response in fluid is a new phenomenon resulting from its structural and biochemical properties. The rheological tests confirmed that the generation of stress in synovial fluid is much more effective than the viscous response. The FEM analysis carried out with rheological experiments may explain the excellent mechanism of temporomandibular joint lubrication.

CONCLUSIONS

Numerical analysis of normal TMJ under load transfer conditions indicates that maximum stresses are located not in the direct friction zone, but in the subchondral structures, cancellous and cortical bones. They are also partially present in the inner zone of the joint disc. It can therefore be concluded that they occur in areas that are remodelled under the influence of compression. The distribution of resultant displacement is strongly differentiated in the structure of the joint. In the bone structures of the zygomatic process, the displacements disappear completely, which may neutralize the influence of the masticatory organ on the skull structures. The presence of displacements with the highest gradient in the lower joint cavity and in the disc structure is characteristic. Slightly less differentiation was found in the upper joint cavity. The highest values of displacement occurred in the posterolateral zone of the head. The cooperation of joint surfaces covered with fibrous cartilage through differential displacement influences the stimulation of the lubrication mechanism and optimization of synovial fluid's rheological parameter use. It is supported by biomechanical forces, controlled by the central nervous system, and implemented by the muscle and ligament

system. Rheological tests carried out on the joint fluid, at variable frequency and constant strain, as well as at variable strain and constant frequency, indicate effective support of the lubrication mechanism by G' conservative module domination, which is a measure of the elastic properties of the liquid. Joint fluid has elastic-viscous properties when the surfaces move relative to each other and when they are loaded. The stimulator of elastic response is a new phenomenon resulting from its structural and biochemical properties. The FEM analysis carried out with rheological experiments may explain the excellent mechanism of TMJ lubrication.

REFERENCES

1. Lippert H., Anatomy. Volume 2. Wrocław: Medical Publisher Urban & Partner, 1998.
2. Ikeda R., Ikeda K.: Directional characteristics of incipient temporomandibular joint disc displacements: A magnetic resonance imaging study. American Journal of Orthodontics and Dentofacial Orthopedics, 149, 1(2016), pp. 39––45.
3. Tappert L., Baldit A., Laurent C., Ferrari M., Lipinski P.: Acquisition of accurate temporomandibular joint disc external shape and internal microstructure. In 8th World Congress of Biomechanics, 2018.
4. Segù M., Manfredini D.: Temporomandibular Joint Disorders in the Elderly. In Oral Rehabilitation for Compromised and Elderly Patients. Springer, Cham., 2019, pp. 63–79.
5. Moreno-Hay I., Okeson, J.P.: Single event versus recurrent luxation of the temporomandibular joint. The Journal of the American Dental Association, 150, 3(2019), pp. 225–229.
6. Tu K.H., Chuang H.J., Lai L.A., Hsiao M.Y.: Ultrasound imaging for temporomandibular joint disc anterior displacement. Journal of medical ultrasound, 26, 2(2018), p. 109.
7. Roberts W.E., Stocum D.L.: Part II: Temporomandibular joint (TMJ) – Regeneration, degeneration, and adaptation. Current Osteoporosis Reports, 16, 4(2018), pp. 369–379.
8. Wei F.: Behavioral, Functional, and Shape Assessment for Temporomandibular Joint, 2018.
9. Balenton N., Khakshooy A., Chiappelli F.: Lubricin: Toward a Molecular Mechanism for Temporomandibular Joint Disorders. In Temporomandibular Joint and Airway Disorders. Springer, Cham, 2018, pp. 61–70.
10. McMillan B.: Wielki Atlas Anatomii Człowieka. Grupa Wydawnicza Foksal, 2013.
11. Barenholz Y., Nitzan D., Etsion I., Schroeder A., Halperin G., Sivan S.: U.S. Patent No. 8,895,054. Washington, DC: U.S. Patent and Trademark Office, 2014.
12. de Moura Silva A., de Figueiredo V.M.G., do Prado R.F., de Fátima Santanta-Melo G., Ankha M.D.V.E.A., de Vasconcellos L.M.R., da Silva Sobrinho A.S., Junior L.N.: Diamond-like carbon films over reconstructive TMJ prosthetic materials: Effects in the cytotoxicity, chemical and mechanical properties. Journal of oral biology and craniofacial research, 9, 3(2019), pp. 201–207.
13. Olsen-Bergem H., Kristoffersen A.K., Bjørnland T., Reseland J.E., Aas J.A.: Juvenile idiopathic arthritis and rheumatoid arthritis: bacterial diversity in temporomandibular joint synovial fluid in comparison with immunological and clinical findings. International journal of oral and maxillofacial surgery, 45, 3(2016), 318-322.
14. Alstergren P.: Rheumatoid Arthritis with Temporomandibular Joint Involvement. In Clinical Cases in Orofacial Pain. Wiley, 2017.
15. Ryniewicz A.M.: Identification, modelling and biotribology of human joints. AGH University of Science and Technology Press, 2011.
16. Ryniewicz A.M., Analiza mechanizmu smarowania stawu biodrowego człowieka. Monografia nr 111, UWND AGH, Kraków 2002.
17. Ryniewicz A.M., Ryniewicz A.: Analiza mechanizmu smarowania stawów człowieka w badaniach in vitro oraz in vivo. Przegląd elektrotechniczny, 90, 5(2014), pp. 142–145.
18. Slavicek R.: The masticatory organ: functions and dysfunctions. GAMMA Medizinisch-wissenschaftliche Fortbildung-AG, 2002.
19. Majewski S.W.: Gnatofizjologia stomatologiczna: normy okluzji i funkcje układu stomatognatycznego. Wydawnictwo Lekarskie PZWL, 2018.
20. Al-Saleh M.A., Alsufyani N.A., Saltaji H., Jaremko J.L., Major P.W.: MRI and CBCT image registration of temporomandibular joint: a systematic review. Journal of Otolaryngology-Head & Neck Surgery, 45, 1(2016), p. 30.
21. Shaik S., Parker M.E.: The assessment of osseous changes in the temporomandibular joint using Cone Beam Computed Tomography. South African Dental Journal, 73, 4(2018), pp. 259–261.

22. Balatgek T.L., Demerjian G.G., Sims A.B., Patel M.: CBCT and MRI of Temporomandibular Joint Disorders and Related Structures. In Temporomandibular Joint and Airway Disorders, Springer, Cham, 2018, pp. 201–218.
23. Ibi M.: Inflammation and Temporomandibular Joint Derangement. Biological and Pharmaceutical Bulletin, 42, 4(2019), pp. 538–542.
24. Liu Z., Qian Y., Zhang Y., Fan Y.: Effects of several temporomandibular disorders on the stress distributions of temporomandibular joint: a finite element analysis. Computer methods in biomechanics and biomedical engineering, 19, 2(2016), pp. 137–143.
25. Shu J.H., Yao J., Zhang Y.L., Chong D.Y., Liu Z.: The influence of bilateral sagittal split ramus osteotomy on the stress distributions in the temporomandibular joints of the patients with facial asymmetry under symmetric occlusions. Medicine, 97, 25(2018), e11204.
26. Ferreira F.M., Cézar Simamoto-Júnior P., Soares C.J., Ramos A.M.D.A.M., Fernandes-Neto A.J.: Effect of Occlusal Splints on the Stress Distribution on the Temporomandibular Joint Disc. Brazilian dental journal, 28, 3(2017), pp. 324–329.
27. Sahoo P., Das S.K., Davim J.P.: Tribology of materials for biomedical applications. In Mechanical Behaviour of Biomaterials. Woodhead Publishing, 2019, pp. 1–45.
28. Wolford L.M., Mercuri L.G., Schneiderman E.D., Movahed R., Allen W.: Twenty-year follow-up study on a patient-fitted temporomandibular joint prosthesis: the Techmedica/TMJ Concepts device. Journal of Oral and Maxillofacial Surgery, 73, 5(2015), pp. 952–960.
29. Mercuri L.G.: Temporomandibular joint total joint replacement – TMJ TJR. Switzerland: Springer Int Pub, 2016.
30. Kerwell S., Alfaro M., Pourzal R., Lundberg H.J., Liao Y., Sukotjo C., Mercuri L.G., Mathew M.T.: Examination of failed retrieved temporomandibular joint (TMJ) implants. Acta biomaterialia, 32, 1(2016), pp. 324–335.
31. Ackland D.C., Robinson D., Redhead M., Lee P.V.S., Moskaljuk A., Dimitroulis G.: A personalized 3D-printed prosthetic joint replacement for the human temporomandibular joint: From implant design to implantation. Journal of the mechanical behavior of biomedical materials, 69(2017), pp. 404–411.
32. Villanueva J., Trino L., Thomas J., Bijukumar D., Royhman D., Stack M.M., Mathew M.T.: Corrosion, tribology, and tribocorrosion research in biomedical implants: progressive trend in the published literature. Journal of Bio- and Tribo-Corrosion, 3, 1(2017), p. 1.
33. Bayer I.: Advances in tribology of lubricin and lubricin-like synthetic polymer nanostructures. Lubricants, 6, 2(2018), p. 30.
34. Mumme M., Barbero A., Miot S., Wixmerten A., Feliciano S., Wolf F., Asnaghi A.M., Baumhoer D., Bieri O., Kretzschmar M., Pagenstert G., Haug M., Schaefer D.J., Martin I., Jacob M.: Nasal chondrocyte-based engineered autologous cartilage tissue for repair of articular cartilage defects: an observational first-in-human trial. The Lancet, 388, 10055(2016), pp. 1985–1994.
35. Musumeci G., Szychlinska M.A., Mobasheri A.: Age-related degeneration of articular cartilage in the pathogenesis of osteoarthritis: molecular markers of senescent chondrocytes. Histol Histopathol, 30, 1(2015), pp. 1–12.